

Original scientific paper

***In vitro* membrane binding and protein binding (IAM MB/PB technology) to estimate *in vivo* distribution: applications in early drug discovery**

Klara Valko*¹, Simon Teague², and Charles Pidgeon³

¹Bio-Mimetic Chromatography, Unit 5B Business & Technology Centre, Stevenage, SG1 2DX Hertfordshire United Kingdom

²GlaxoSmithKline, Stevenage, United Kingdom

³Independent Researcher, affiliate of Regis Technologies Inc, Morton Grove, IL 60052 USA

*Corresponding Author: E-mail: Klara_Valko@bio-mimetic-chromatography.com; Tel.: +44-7521989558;

Received: February 07, 2017; Revised: March 14, 2017; Published: March 25, 2017

Abstract

The drug discovery process can be accelerated by chromatographic profiling of the analogs to model *in vivo* distribution and the major non-specific binding. A balanced potency and chromatographically determined membrane and protein binding (IAM MB/PB) data enable selecting drug discovery compounds for further analysis that have the highest probability to show the desired *in vivo* distribution behavior for efficacy and reduced chance for toxicity. Although the basic principles of the technology have already appeared in numerous publications, the lack of standardized procedures limited its widespread applications especially in academia and small drug discovery biotech companies. In this paper, the standardized procedures are described that has been trademarked as Regis IAM MB/PB Technology®. Comparison between the Drug Efficiency Index ($DEI = pIC_{50} - \log V_{du} + 2$) and generally used Ligand Lipophilicity Efficiency (LLE) has been made, demonstrating the advantage of measured IAM and HSA binding over calculated log P. The power of the proposed chromatographic technology is demonstrated using the data of marketed drugs.

Keywords

Drug efficiency; Biomimetic properties by HPLC; unbound volume of distribution; *in vivo* distribution

Introduction

Medicinal chemists face multi-factorial challenge problems when designing drug molecules that can reduce the impact or cure a pathological condition; drug discovery scientists seek the smallest possible dose with minimal side effects [1-4]. Screening cascades often generate vast quantities of primarily *in-vitro* data, and in some cases, *in vivo* data on compounds that form a decision on which compounds are selected for further progression. This paper documents an alternative screening triage which can help to avoid the problem of analysing too much discovery data when choosing lead compounds to pursue.

Chemical structure design of discovery molecules usually focuses on elucidating the structure – activity relationships after identifying the target enzyme/receptor followed by the development of a potency screening method. The active molecules are then tested for a variety of assays for affinity and

developability, such as enzyme assays, selectivity assays, cellular assays, CaCo2 or MDCK cell permeability, solubility [5], lipophilicity, microsomal stability, Hep G cell hepatotoxicity, cellular toxicity, [6] etc. All future reference to receptors will have dual meaning referring to either receptor or enzyme targets, for simplicity.

Project teams usually design screening cascades to guide the filtering process of compounds after each measurement, to ensure those compounds that do not meet pre-defined criteria in a particular assay are eliminated from further screening. This sequential screening process frequently excludes compounds with good *in vivo* drug properties; marketed drugs have appropriate *in vivo* properties for the disease they are being developed to treat, along with sufficient potency to engage the target and produce the desired effect. The discovery challenge is to recognise that discovery compounds may exhibit high potency, but they may lack acceptable *in vivo* distribution enabling the compound to achieve a therapeutic free drug concentration at the target receptor in the target tissue(s) *in vivo*. *In vivo* properties, particularly distribution, are as important as high potency or receptor occupancy. Regardless of this fact, none of the properties which are typically measured during compound screening is on their own sufficient to predict the compound's fate *in vivo* or in human clinical trials. This must ultimately be measured. Several other properties should also be measured, which include target binding, selectivity, absorption, distribution, metabolism and elimination (ADME), pharmacokinetics and pharmacodynamics (PK/PD) profile, and of course the safety profile.

In order to find good absorption and bioavailability, chemists have to design molecules which will have good solubility and permeability, and in general lipophilicity. Designing a drug candidate which has good clinical ADME properties, is often much different than designing discovery compounds with simply high receptor binding or potency. Various ligand efficiency parameters have been introduced and frequently used by medicinal chemists that relate the measured potency to some calculated properties of the compounds such as, size and lipophilicity as it has been recently reviewed [7-8]. This manuscript describes how chromatographic analysis can efficiently predict or help select which compounds have the greater probability of becoming lead molecules by balancing the receptor binding or potency with optimum compound distribution *in vivo*.

Obviously, achieving good oral absorption alone is not sufficient when choosing a drug candidate. Overcoming the body's natural defense mechanisms is also necessary to achieve relevant oral bioavailability as nature has evolved animal and human protection against potentially harmful xenobiotics. Some of these defense mechanisms we need to consider when developing NCE's are: (i) gut metabolism, (ii) efflux processes and (iii) first pass metabolism. Thus, ensuring that discovery molecules are not subject to active efflux and quick elimination or metabolism is current mainstream thinking in most drug discovery processes.

The latest studies show that the most significant problem with the late-stage attrition of discovery molecules is related to safety and efficacy. Many safety-related issues have been directly attributed to the lipophilicity of compounds [9-12] especially when it is measured using Immobilized Artificial Membranes (IAMs). High IAM binding is indicative of the compound's binding to multiple targets or receptors, this is often referred to as compound promiscuity. This may cause unwanted pharmacology or toxicity. It has previously been shown that compounds that require lower clinical dose (ranging between 1-100 mg) and therefore lower efficacious plasma concentrations are less likely to cause toxicity [9,13].

The root cause of these problems is partially dominated by the compounds binding or partitioning into tissue which is predominantly comprised of membrane phospholipids; when this happens, the drug is sequestered into non-specific phospholipid binding sites and is then less available as a free drug near the

target of interest. Plasma proteins can also reduce the amount of free drug available to interact with enzymes/receptors (and when this happens an increased dose is essential). Thus, the non-specific binding/partitioning of compounds to phospholipids and proteins reduce the available free concentration at the site of action. Thus, increased doses are needed for activity, but, this increases the possibility of undesired pharmacology or toxicity.

This paper focuses on the role of distribution in the Absorption, Distribution, Metabolism and Elimination (ADME) process, without neglecting the absorption and clearance that regulate the magnitude and the frequency of dosing. We propose to design and triage NCEs based on their *in vitro* distribution behavior that determines the amount/concentration of compounds in various tissue compartments, and the free unbound compartments that are responsible for safety issues and efficacy, respectively. This can be achieved by using some of the major protein components which make up tissues in the body as chromatographic stationary phases, this is called biomimetic chromatography and has been recently reviewed [14].

We also propose that the unbound volume of distribution of compounds is an important parameter to consider, as this *in vivo* parameter describes the proportion of the dose relative to the free plasma concentration of compounds in steady state [15]. Based on the free drug hypothesis, [16] the free plasma concentration is the same as the free tissue concentration, when no permeability barrier or active transport distorts the thermodynamic equilibrium, between plasma and tissues which contain the therapeutic targets. Though active transporters may have a significant effect on the free concentration of a drug on the two sides of the membrane [17], the concentration difference can be explained by strong binding of the drug to intracellular components. The free concentration difference is usually not more than an order of magnitude on the two sides of the membrane due to active transporters that require constant energy supply to keep the concentration difference. Distorting the thermodynamic equilibrium by two to three orders of magnitude would require constant energy supply (ATP), and the active transporters may become easily saturated.

The unbound volume of distribution can be considered as a proportional parameter to the drug partition coefficient between the free and bound compartments. In this respect, it is very similar to the recently introduced drug efficiency parameter that relates the free bio-phase concentration to the dose. The drug efficiency concept that was introduced by Braggio [18] highlights the importance of the free concentration of the drug in the biophase near the target relative to the dose to achieve efficient PK/PD of a drug molecule. The drug efficiency index, DEI highlights the importance of balancing the potency and drug efficiency of the molecules and is proposed as an alternative parameter to simply focusing on potency, as other ligand efficiency parameters tend to be biased towards [19]. The DEI concept also helps designing drug molecules with a low therapeutic dose that in turn reduce general toxicity.

Table 1 shows the abbreviations and their meaning of the properties that are investigated in this paper, while Table 2 shows the equations how they are calculated and how they are related to each other.

The drug distribution properties are most often characterised by lipophilicity. Lipophilicity has been recognised for a long time as the principal parameter that influences solubility [20,21], permeability [22], tissue binding, protein binding [23,24], toxicity [10], promiscuity [1], clearance [25] etc. Several ligand efficiency parameters contain the lipophilicity and propose to consider the potency relative to the lipophilicity of the compounds, such as Ligand Lipophilicity Efficiency, LLE [7,26]. Recently, the chromatographic lipophilicity has been combined with the number of aromatic rings in the molecules to derive the Property Forecast Index (PFI) [27]. It has been suggested that having a PFI value less than 6 for

drug discovery compounds increases the probability of improving drug attrition rates.

Table 1. Variables, abbreviations used throughout the text

IAM	Immobilized Artificial Membrane (HPLC stationary phase_
HSA	Human Serum Albumin
AGP	Alpha-1-acid-glycoprotein
PPB	Total plasma protein binding
MB	Membrane Binding (measured by IAM)
MB/PB	Membrane binding and protein binding
V_{dss}	Steady state volume of distribution (dose/plasma concentration)
V_{du}	Steady state unbound volume of distribution (dose/free plasma concentration= V_d/f_u)
f_u	Unbound fraction in plasma
DE	Drug efficiency (100* free biophase conc/dose)
DE_{max}	Drug efficiency measured by MB/PB by HPLC (100*free plasma conc/dose)
DEI	Drug efficiency index, potency plus log DE_{max} (pIC50 +log DE)
IAM MB	Membrane binding index, previously known as CHI(IAM)
clogP	Calculated logarithm of octanol/water partition coefficient
Log D/P	Logarithm of distribution/partition coefficient

Table 2. Equations used to predict distribution properties

log $K(IAM)$; Eq. (1)	$= 0.29 * e^{(0.026MB+0.42)} + 0.7$
log $K(HSA)$; Eq. (2)	$= e^{\log k(HSA)}$
log $k(HSA)$	$= \log(\%HSA_{bound}/(101 - \%HSA_{bound}))$
Estimated log V_{dss} ; Eq. (3)	$= 0.44 * \log K(IAM) - 0.22 * \log K(HSA) - 0.62$
Estimated log V_{du} ; Eq. (4)	$= 0.23 * \log K(HSA) + 0.43 * \log K(IAM) - 0.72$
DE_{max} ; Eq. (7)	$= 100/V_{du}$
LLE	Ligand lipophilicity efficiency (pIC50 -clogP)
log $k(PPB)$ (8)	$0.87 * \log k(HSA) + 0.17 * \log k(AGP) + 0.06 * cMR - 0.27$

Lipophilicity has been historically characterised by the octanol/water partition coefficient, log P , for the neutral form of the molecules and by the distribution coefficient, log D , measured at different pHs, mainly at pH 7.4. Log P is widely used since the work of Hansch [28] who suggested log P to describe the so-called “random” walk of the drug molecule that reduces its free concentration near the receptor. Lipophilic compounds energetically do not favour residing in the aqueous environment and have a preference to “stick” to any hydrophobic surface in the body. The octanol/water system is able to partially mimic the polar groups with hydrogen bond donor and acceptor properties that may be present in the lipophilic environment in the body and therefore serve as a good model to describe biological distribution. However, the octanol/water lipophilicity and any other lipophilicity measure that does not include cellular membranes and proteins, fails to explain the biological distribution of molecules when they have charge or special shape. An example is the comparison of nifedipine and amlodipine (see Figure 1). Nifedipine is more lipophilic at physiological pH but still, the volume of distribution of amlodipine is 30 times higher, indicating 30 times higher partitioning to tissues than nifedipine. The clearance of nifedipine is 9.8 mL/min/kg [29], and clearance of amlodipine is in a similar range, 7 mL/min/kg [30]. The major difference between the two

molecules is a basic amine group on amlodipine. The basic group results in amlodipine having a stronger binding to phospholipids than albumin, and this results in a large difference in their volumes of distribution.

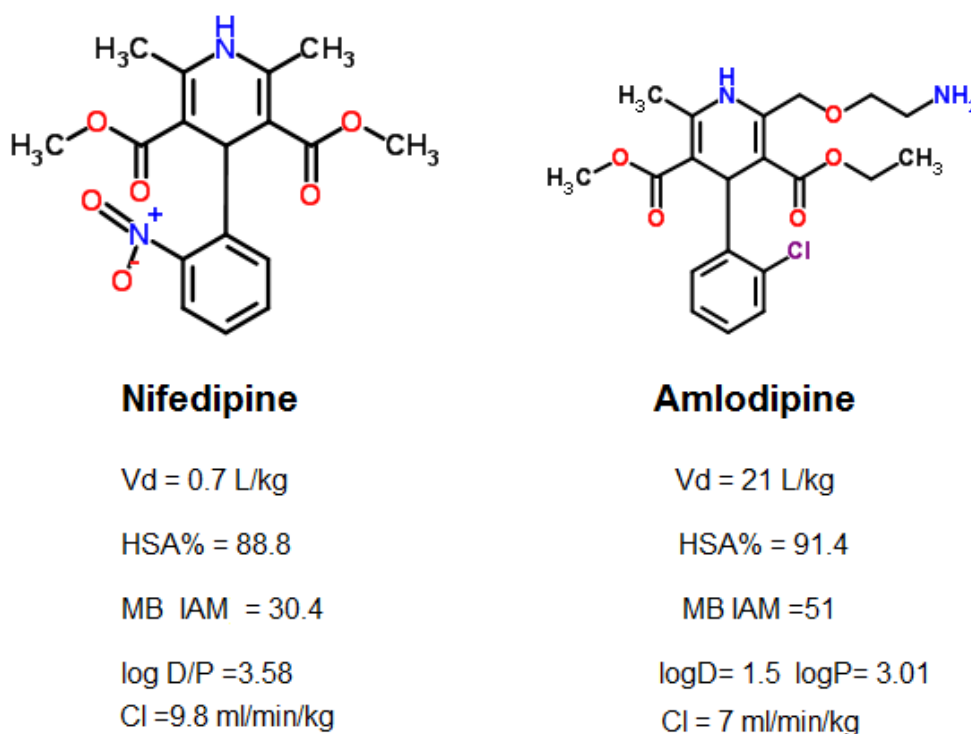


Figure 1. Physico-chemical and biomimetic properties of nifedipine and amlodipine

Besides measuring the octanol/water partition coefficients we propose a method of measuring the protein and phospholipid binding of the compounds using reverse phase high-performance liquid chromatography in conjunction with the Membrane Binding/Protein Binding Technology (MB/PB Technology®) registered to Regis Technologies inc. Using this approach, we can measure compounds interaction with phosphatidylcholine membrane (IAM), human serum albumin (HSA) and alpha-1-acid glycoprotein (AGP). These are commercially available HPLC stationary phases that contain or mimic these constituents of the body. These include (i) IAMs, (ii) chiral HSA and (iii) chiral AGP.

The IAM concept was introduced by Pidgeon et al. [31-33] and it was the first attempt to emulate the biological membrane on a solid surface. HPLC columns with IAM stationary phase where the phosphatidylcholine moiety is chemically bonded to a solid surface mimic the density of phosphatidylcholine in the biological membrane bi-layer. Other approaches do exist for measuring membrane binding such as using liposome partition measurements or micellar electrophoresis [35-36]. However, they have their limitations and are also very time-consuming. Biomimetic stationary phases have been validated by comparing the retention times obtained on the commercially available ChiralPak-HSA [37-39] and ChiralPak-AGP [40-41] stationary phases result in binding values that are proportional to the albumin and AGP binding of compounds obtained by equilibrium dialysis. When using biomimetic stationary phases the retention time of the compounds is directly proportional to the dynamic equilibrium constant between the mobile phase (buffer at physiological pH) and the actual body component (membrane and proteins) in the stationary phase. The process is very similar to the biological distribution processes that are also dynamic (never in real equilibrium unless at steady state) and occurs on the surfaces of the biomimetic stationary phases. The measured membrane binding parameters reflect the three-dimensional nature of the molecule's interaction within an *in vivo* system (the drug, membrane and protein

stationary phase) that has been demonstrated in the literature [14]. The chromatographic technique to measure these biomimetic properties has several other technical advantages. It can be easily automated; there is no need for concentration determination and measurements. The important thing is, however, to standardise the retention times and binding data by measuring a calibration set of compounds with each compound set to be able to get normalised retention times for each of the stationary phases being used to generate binding data (IAM, HSA and AGP). A detailed description of the standardised methodology for each of the IAM MB/PB stationary phases has recently been published [14].

There are several publications establishing the usefulness of the IAM MB/PB technology to model *in vivo* drug distribution, such as the volume of distribution model [42], unbound volume of distribution model [43-44] and how they can be used to screen compounds in early drug discovery [45]. It was found that strong IAM MB (CHI IAM > 50) can be related to phospholipidosis [46-47], as well as high volume of distribution and tissue partitioning [43]. Recently, it was found that promiscuity (i.e., a discovery compound binding to multiple receptors) showed good correlation to the IAM MB of drug discovery compounds. The IAM MB data showed a good correlation with the intracellular concentration of compounds, indicating that membrane binding is important to get compounds into the cell [48]. Estimating the potential clinical dose as early as possible is an important aspect of the drug discovery process to help select the optimal compound profile and highest probability of successful progression to the clinic [49-50]. Valko et al. [51] highlighted that the maximum achievable drug efficiency (DE_{max}) that can be obtained assuming (i) 100 % bioavailability, (ii) no permeability barrier and (iii) no active transport could be calculated using *in vitro* biomimetic measurements, essentially the Regis IAM MB/PB Technology[®] that we are proposing in this paper as a useful tool in early drug discovery [51]. The drug efficiency concept as a design parameter has the advantage that it can be estimated from *in vitro* measurements, and can be monitored during the drug development process to see how the early estimation performs when *in vivo* measurements become available pre-clinically, or from human clinical trials. In this paper, the intention is to show the models and the applicability of the Regis IAM MB/PB Technology[®] in early drug discovery. It is also important to have the ability to estimate these *in vitro* properties from the chemical structure thus helping the design stage of the molecules too. It has been shown that the retention of compounds obtained on the proposed biomimetic stationary phases can be estimated *in silico* [52-55], however it is worth noting that the *in silico* models use 2D molecular descriptors that are not sufficient to estimate the 3D contribution of the molecules binding to proteins, therefore they can be used only as a rough estimations.

Phospholipids constitute approximately 40 % of the human body, therefore, the phospholipid binding of compounds are a very important parameter that should not be ignored in the drug design process. It was found that MB IAM values above 50 indicate promiscuous binding [57], and higher phospholipidotic potential [56-59] for discovery compound. It was also found that MB IAM showed a good correlation with the total cellular concentration of discovery compounds [60].

In this paper, we present the models for human clinical unbound volume of distribution and drug efficiency using measured biomimetic properties, and we describe a protocol how to use these data in early lead optimisation.

Experimental

The values for dose, potency (pIC₅₀), the volume of distribution, clearance, the half-life of the known drugs were obtained from various databases (www.drugbank.ca/drugs and www.drugs.com) and listed in Table A1. The measured IAM MB/PB data are published in the book by Valko [45] and listed in Table A2. Table A2 contains the estimated volume of distribution (IAM MB/PB log V_{dss}) and the estimated unbound

volume of distribution (IAM MB/PB $\log V_{du}$) using the published models [42-43], and the Regis IAM MB/PB Technology®. The same technology has been applied to estimate the Maximum Drug Efficiency (HPLC DE_{max}) value, that represents the maximum drug efficiency that can be achieved when the bioavailability is 100 %, and there is no permeability barrier or active transport to disturb the steady state equilibrium. This can be expressed as the reciprocal value of the steady-state unbound volume of distribution [51].

The IAM MB data were obtained using IAM PC.DD2 HPLC column (Regis Technologies, Inc., IL, USA) with the dimensions of 100 x 3 mm. Mobile phase A was 50 mM ammonium acetate adjusted to pH 7.4, while mobile phase B was 100 % acetonitrile. The flow rate was 1.5 mL/ min, the linear gradient was 0 to 80 % acetonitrile in 0 to 5 min, 5 to 5.25 min 80 % acetonitrile then back to 0 % acetonitrile by 5.5 min. The total run time is 7 min. The calibration set of compounds are listed in Table 3 and the calibration test solution is available from Bio-Mimetic Chromatography, UK (www.bio-mimetic-chromatography.com). A typical chromatogram is shown in Figure 2.

It is essential to obtain a straight line between the retention times and the IAM MB index of the calibration set of compounds. Moreover, it is essential to run a system suitability test of compounds (2 neutral, 2 basic and 2 acidic compounds) listed in Table 4, and check that the measured IAM MB data are the same +/- 5 units listed in the table. This ensures that the IAM phospholipid immobilised phase is maintained, preserving the natural phospholipid density on the column.

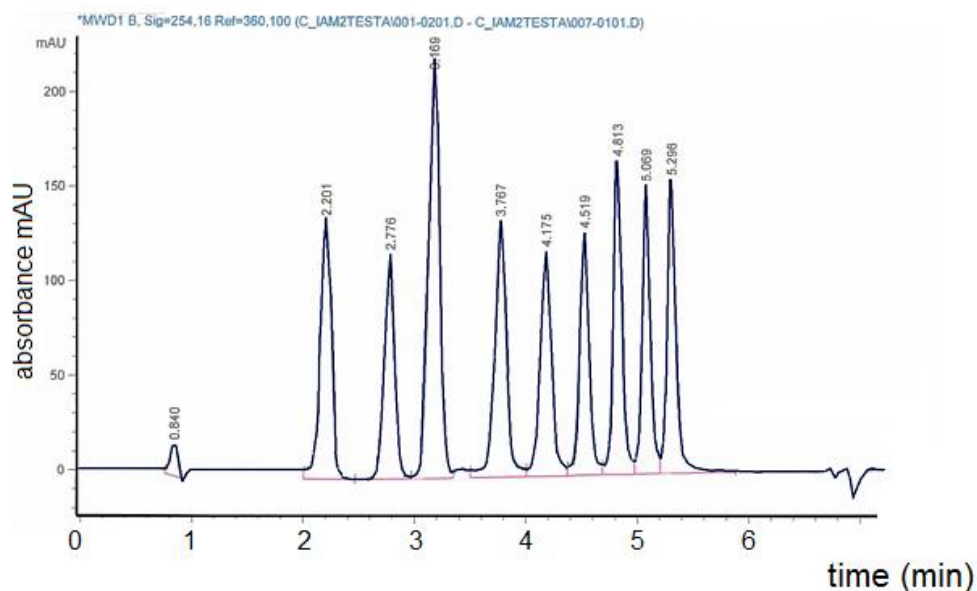


Figure 2. A typical chromatogram obtained on IAM PC.DD2 100 x 3 mm HPLC column. Flow rate: 1.5 mL/min, mobile phase A; 50 mM ammonium acetate adjusted to pH 7.4, B: acetonitrile. Run time 7 min; Gradient: 0 to 5 min 0 to 80 % B, 5 to 5.25 min 80 % B, 5.25 to 5.5 min 0 % B

It was found that the $\log k(\text{IAM})$ shows a non-linear relationship with $\log P$ octanol/water values [42]. To convert the $\log k(\text{IAM})$ scale to the $\log P$ scale we need the transformation as shown by equation (1). The converted $\log K(\text{IAM})$ data is equivalent to the partition coefficient of the compound between the pH 7.4 buffer and the phospholipid phase.

$$\log K(\text{IAM}) = 0.29 * e^{(0.046 * \text{MB IAM} + 0.42)} + 0.70 \quad (1)$$

This data are then be used in the models for the volume of distribution, unbound volume of distribution and the *in vitro* maximum drug efficiency (HPLC DE_{max}).

Table 3. The calibration set of compounds and their standard IAM MB score on IAM.PC.DD2 column. The IAM MB data approximate to the acetonitrile concentration in the mobile phase when the compound elutes using the gradient conditions. The $\log k(\text{IAM})$ values obtained as $0.046\text{IAM MB}+0.42$ where the constants have been derived by plotting isocratic $\log k(\text{IAM})$ data extrapolated to 0 % acetonitrile mobile phase using isocratic measurements [52].

Compound	Typical t_R (min)	IAM MB	$\log k(\text{IAM})$
Octanophenone	3.18	49.4	2.69
Heptanophenone	3.07	45.7	2.52
Hexanophenone	2.94	41.8	2.34
Valerophenone	2.79	37.3	2.14
Butyrophenone	2.58	32	1.89
Propiophenone	2.35	25.9	1.61
Acetophenone	2.04	17.2	1.21
Acetanilide	1.85	11.5	0.95
Paracetamol	1.62	2.9	0.55

Table 4. System suitability test compounds and their expected IAM MB data. The measured values should be within 5 IAM MB value agreements with the values in the table. Further drug molecules data can be found in reference [45].

Compound	Acid/base	IAM MB
Carbamazepine	Neutral	26.5
Colchicine	neutral	18.0
Warfarin	Acidic	16.0
Indomethacin	Acidic	24.5
Nicardipine	Basic	45.1
Propranolol	Basic	46.8

The PB data are obtained on Chiralpack-HSA and ChiralPack AGP columns with the dimensions of 50 x 3 mm. The flow rate was 1.5 mL/min and 2-propanol was used as mobile phase B, while mobile phase A is 50 mM ammonium acetate adjusted pH to 7.4. The calibration set of compounds and their $\log k(\text{HSA})$ and $\log k(\text{AGP})$ data are listed in Table 5a and 5b. These data are derived from literature %HSA and %AGP binding data obtained by other methodology (equilibrium dialysis and ultrafiltration). These data are used to calibrate the gradient retention times on the protein column so that the binding data obtained from the retention times are comparable with binding data obtained by other methodologies. The typical retention times were obtained using a 6 min gradient run: 0 to 3 min 0 to 35 % 2-propanol, 3 to 4 min 35 % 2-propanol, 4 to 4.2 min back to 0 % 2-propanol. Typical calibration plots and chromatograms have been published previously [14]. It was found that the obtained $\log k(\text{HSA})$ showed a non-linear relationship with the $\log P$ values of acetophenone homologues [42]. To convert the $\log k(\text{HSA})$ data to the $\log P$ scale we need to transform them using Equation 2. The so obtained $\log K(\text{HSA})$ data are used in the models.

$$\log K(\text{HSA}) = e^{\log k(\text{HSA})} \quad (2)$$

The published *in vivo* models used the above-described MB/PB data using the following equations below:

$$\text{MB/PB } \log V_{\text{dss}} = 0.44 * \log K(\text{IAM}) - 0.22 * \log K(\text{HSA}) - 0.66 \quad (3)$$

$n=179 \quad r^2=0.76 \quad s=0.33$

where MB/PB $\log V_{dss}$ is the estimated *in vivo* steady state volume of distribution based on 179 known drugs human clinical data [42].

The model for the unbound volume of distribution has also been published previously using the available data for 70 marketed drugs [43] and shown by Equation 4.

$$\text{MB/PB } \log V_{du} = 0.23 \log K(\text{HSA}) + 0.43 \log K(\text{IAM}) - 0.72 \quad (4)$$

$n=70 \quad r^2=0.84 \quad s=0.32$

The HPLC DE_{max} data were calculated using the reciprocal value of the MB/PB $\log V_{du}$ data and validated against human clinical DE_{max} data [51].

Table 5. The literature % binding data and the $\log k(\text{HSA})$ (a) and $\log k(\text{AGP})$ (b) data for the calibration set of compounds. The logarithmic retention times measured under a given condition should result in a straight line when plotted against the $\log k$ data. The regression coefficient should be above 0.96 and the warfarin enantiomers should be baseline separated in order to pass the suitability of the column for protein binding determination.

(a)

Bio-Mimetic Chromatography calibration set of compounds	Typical t_R (min)	$\log t_R$	% HSA from literature plasma protein binding	$\log k(\text{HSA})$ (as $\log(\% \text{HSA}/(101-\% \text{HSA}))$)
Warfarin	3.267	0.51	97.90	1.50
Paracetamol	0.285	-0.55	14.00	-0.79
Nizatidine	0.293	-0.53	20.40	-0.60
Trimethoprim	0.512	-0.29	37.60	-0.23
Propranolol	0.895	-0.05	66.60	0.29
Carbamazepine	1.216	0.08	75.00	0.46
Nicardipine	2.374	0.38	95.00	1.20
Indomethacin	4.117	0.61	99.50	1.82
Diclofenac	3.879	0.59	99.80	1.92

(b)

Bio-Mimetic Chromatography calibration set of compounds	Typical t_R min	$\log t_R$	%AGP (obtained by ultrafiltration [45])	$\log k(\text{AGP})$ (expressed from %AGP as $\log(\% \text{AGP}/(101-\% \text{AGP}))$)
Warfarin	3.72	0.57	83.2	0.67
Acetaminophen	1.16	0.06	3.2	-1.49
Nizatidine	2.19	0.34	37.1	-0.24
Trimethoprim	2.50	0.40	46.2	-0.07
Propranolol	3.86	0.59	86	0.76
Carbamazepine	3.21	0.51	73.2	0.42
Nicardipine	4.08	0.61	92	1.01
Indomethacin	2.98	0.47	52.9	0.04
Diclofenac	3.09	0.49	69.3	0.34

For the calculation of the stepwise regression equations, the academic version of JMP (SAS Institute) software has been used. The calculation of the physicochemical parameters the Chemaxon and ACD software were used. For creating the plots the Sentira version 1.0.0.6 (Optibrium 2014) software has been used.

Results and discussion

The importance of the unbound volume of distribution and the drug efficiency in the drug discovery process has been discussed in several recent papers focusing on the clearance and plasma protein binding [15-16]. There is a general consensus that the free concentration of the compound at the site of action drives clinical efficacy together with the high affinity for the target receptor. However, a significant debate remains regarding what determines the free concentration; the dose, dosing frequency, intrinsic clearance, plasma protein binding or volume of distribution, all are important factors that should be considered. We can depict a simplified model as it was described by Stepensky [15,61] and consider that the dosing amount and frequency required to balance the elimination rate of a compound determines the amount of drug in the body. While the volume of distribution describes how the total amount of drug distributes between the tissue and plasma compartment, unbound volume of distribution describes the drug distribution between the free and bound compartments regardless of the location where the drug binds (tissues or plasma proteins, see Figure 3).

While investigating known drugs it was clear that the volume of distribution showed no correlation alone to clearance or half-life. However, it did show a good correlation with the product term (or the sum of their logarithmic values clearance and half-life) as is shown in Figure 4a, b and c. The data supports the statement that the distribution properties of compounds are an independent parameter from the clearance.

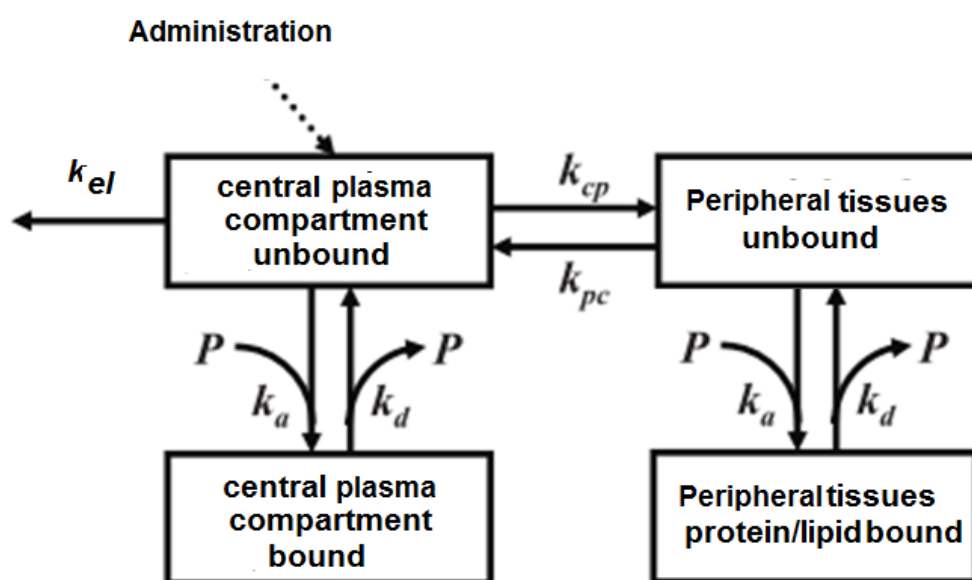


Figure 3. The schematic absorption, distribution and elimination process

The tissue/plasma partition coefficient of a compound can be defined as the tissue concentration divided by the plasma concentration of the compounds. The concentration can be expressed as the amount of drug in the tissue and plasma volume respectively, so $K_{\text{tissue/plasma}}$ can be described by Equation 5:

$$K_{\text{tissue/plasma}} = \frac{(\text{Dose} - A_p)/V_t}{A_p/V_p} \quad (5)$$

where the amount of drug in tissues equals the dose minus the amount in plasma (A_p), V_t is the tissue volume, V_p is the plasma volume. As the steady-state volume of distribution (V_{dss}) equals the dose over the

plasma concentration, introducing that into Equation 5 we can express the tissue plasma partition as a proportionality term to the steady state volume of distribution shown in Equation 6.

$$K_{tissue/plasma} = \frac{V_{dss} - V_p}{V_t} \quad (6)$$

In turn, the volume of distribution of marketed drugs could be modeled by the difference in the membrane and the protein binding of compounds as described by Equation 3 and shown in Figure 5 for the investigated compounds. There are only 40 compounds that have been included in the training set, the majority of the compounds were not included in the original model. That explains that the statistics are slightly worse ($r^2 = 0.76$; root mean square error = 0.33 in the original model, while here the $r^2 = 0.57$ and root mean square error = 0.40).

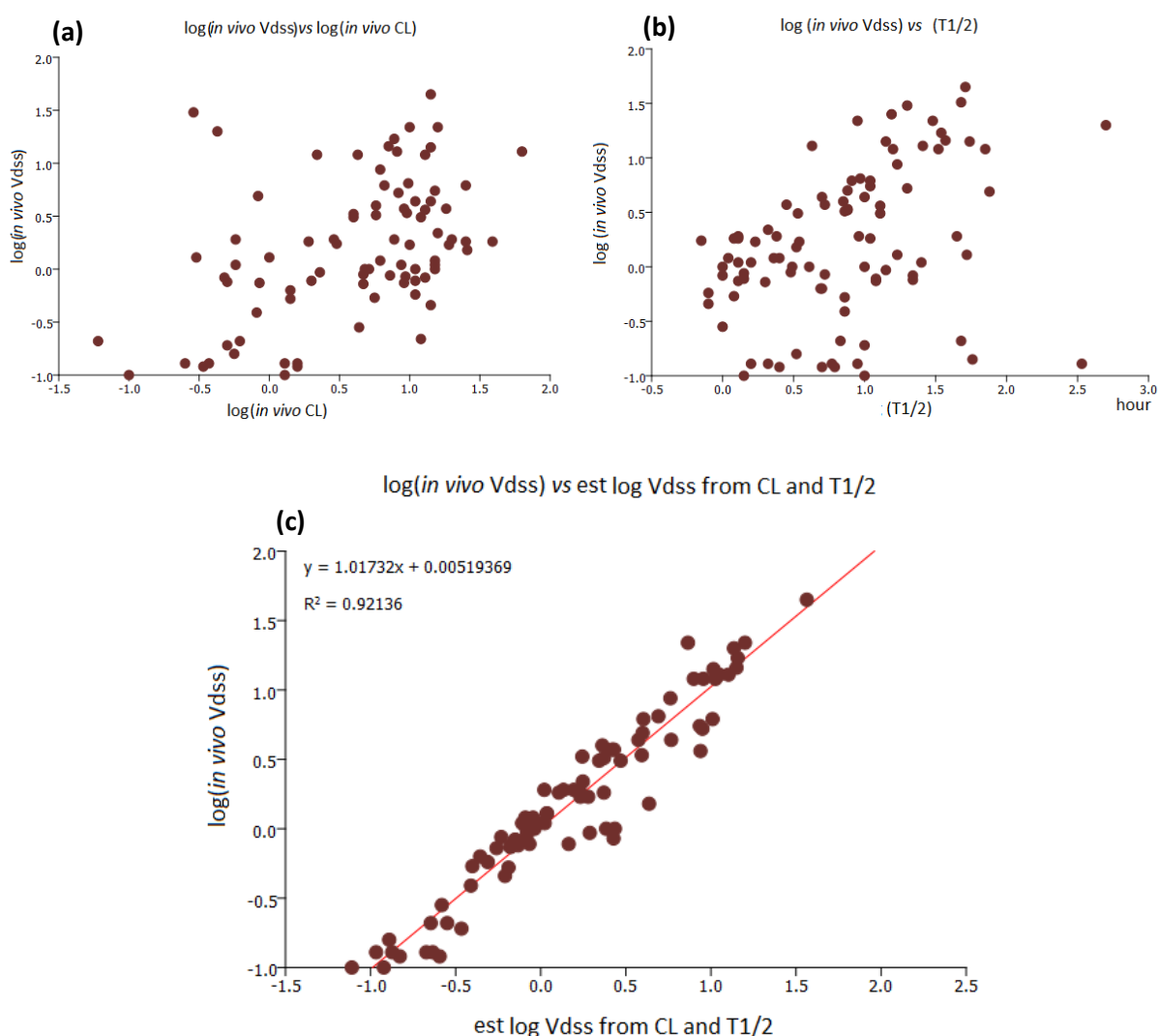


Figure 4. The plot of $\log V_{dss}$ vs \log in vivo CL (a), $\log V_{dss}$ vs $\log T_{1/2}$ (b) and $\log V_{dss}$ vs the sum of $\log CL$ and $\log T_{1/2}$.

The unbound volume of distribution is in principle the reciprocal value of the maximum drug efficiency (DE_{max}) defined by Braggio et al. [18], that is defined by the proportion of the free bio-phase concentration and the dose. If the free drug hypothesis is true, which means the free plasma concentration is similar to

the free tissue concentration of the compounds when no permeability barrier or active transport distorts the equilibrium, then the model for the unbound volume of distribution can be used to estimate the maximum drug efficiency (DE_{max}) of the compounds. Based on the definition of the V_{du} and DE_{max} , their relationship can be described by Equation 7.

$$DE_{max} = \frac{100}{V_{du}} \quad (7)$$

Figure 6 shows the unbound volume of distribution and the estimated DE_{max} of the marketed drugs listed in Table A1. In this case, only 10 compounds overlapped with the original training set. Most of the compounds can be considered as a test set. The root-mean-square error increased from 0.32 to 0.45 while the r^2 dropped from 0.84 to 0.66. The statistics for the training set is $r^2 = 0.76$ and the standard error of the estimate is $s = 0.33$. The estimates can be considered as very predictive, as we have just used two major binding components in the body to describe the total non-specific binding of the compounds to the phospholipids and albumin type of proteins.

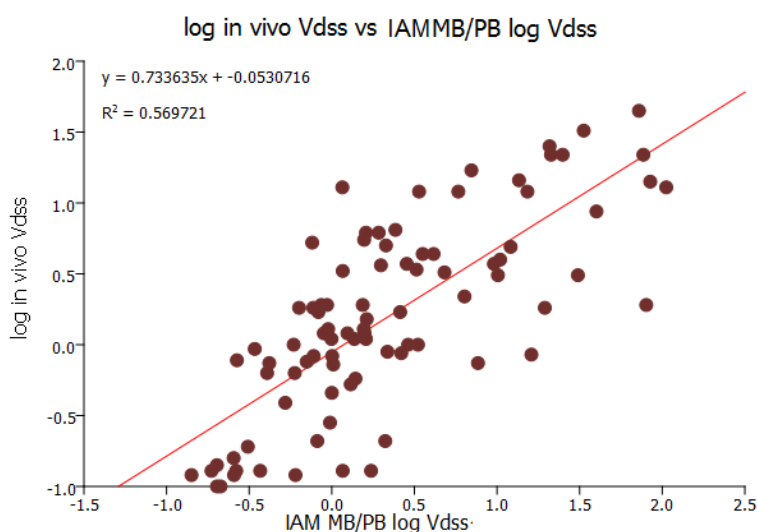


Figure 5. The observed in vivo $\log V_{dss}$ vs the estimated V_{dss} by the IAM MB/PB Technology® using Equation 3.

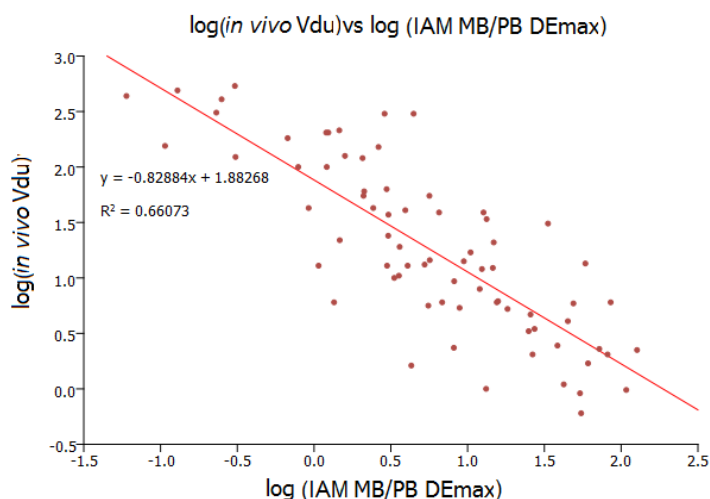


Figure 6. The plot of the human unbound volume of distribution and the estimated DE_{max} using the IAM MB/PB technology and Equation 4.

It is interesting to observe that the estimated DE_{max} of the marketed drugs is typically 1 % or just above. This also means that the unbound volume of distribution of marketed drugs is typically less than 100 L/kg. Thus, when we plot the potency (pIC_{50}) values in the function of the Drug Efficiency Index (DEI), which is the sum of the pIC_{50} and the $\log DE$, the marketed drugs are around the line of unity (see Figure 7). It has been observed [51] that discovery compounds usually have very narrow potency range (pIC_{50} between 7 to 9), but a much broader range of drug efficiency index. Based on the retrospective analysis it turned out that compounds that are on the right side of the line of unity survived the strict candidate selection procedure and showed a good PK/PD profile [51].

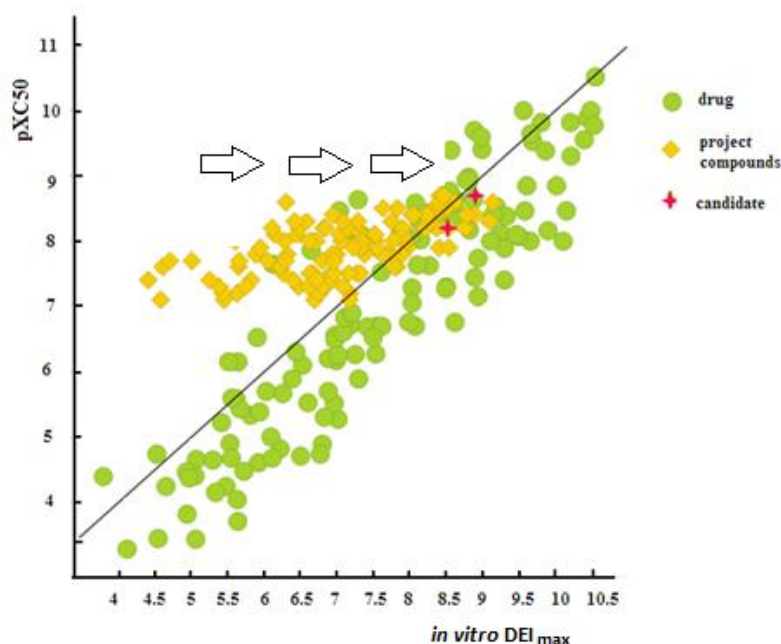


Figure 7. The plot of potency in the function of DEI. The line of unity represents when the drug efficiency $DE=1\%$. The logarithm of 1 is zero, thus, $DEI = pIC_{50}$. The yellow squares show project compounds [51], having the same good potency but a range of DEI. The candidate molecules (red stars) are on the right-hand side of the line where most of the marketed drugs are.

It is interesting to note that we could not find any marketed drugs with drug efficiencies higher than 10-15 %. This suggests that there should be an optimum proportion of the dose and free bio-phase concentration that is less than 10-15 % drug efficiency. It is very likely, that when the high proportion of the administered amount of compound is free then the elimination rate/clearance will be high and the various total tissue concentrations may be low. Therefore, we can optimise drug discovery compounds and triage them to have reasonably good potency if the drug efficiency is approximately 1 to 5 %.

The Regis IAM MB/PB Technology® that use biomimetic HPLC stationary phases to measure the dynamic equilibrium constants of the compounds with the major binding components of the body enables the estimation of volume distribution and unbound volume of distribution without using *in vivo* experimentation for the fraction of the cost and time.

It is also interesting to note that the DE_{max} values representing the sum of the albumin and phospholipid binding showed very good inverse correlation with $\log P$ (much better than with $\log D$) [51]. This is because the $\log D$ drops whatever charge is present on the molecule at pH 7.4, however the sum of albumin and phospholipid binding change very little with the presence of charge. It is because positively charged compounds bind more strongly to IAM (phospholipids) while negatively charged compounds have

a stronger affinity to albumin type of proteins. That is why $\log P$ is a better model to use than $\log D$ [51]. Therefore, there is a connection between DEI and LLE. DE_{\max} determined by the IAM MB/PB Technology is a better representation of the nonspecific binding of the compounds than $\log P$ as it is based on real albumin and IAM affinity of the compounds. In our earlier paper, we have shown that IAM MB/PB DE_{\max} showed a better correlation with *in vivo* $\log DE_{\max}$ than LLE as it shown in Figure 8a and 8b.

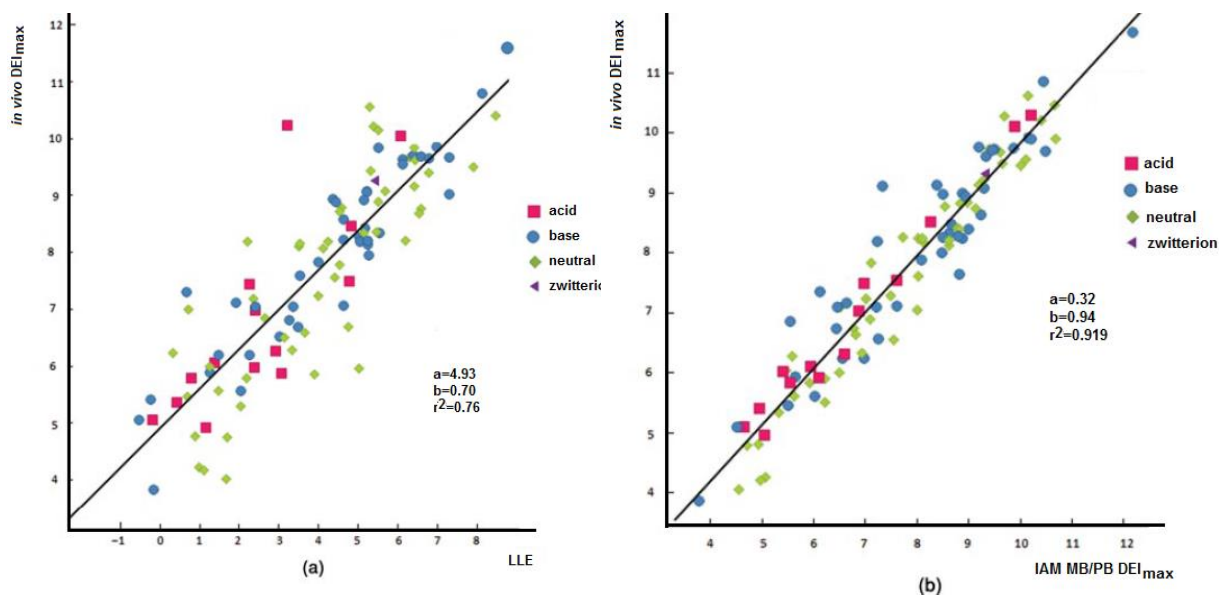


Figure 8. Comparison of the relationship between *in vivo* $\log DE_{\max}$ vs LLE (a) and IAM MB/PB $\log DE_{\max}$ (b), respectively based on the analysis in reference [51].

The better fit is not surprising, as $\log P$ was intended to model the non-specific binding in the body caused by lipophilicity of the compounds. The IAM MB/PB technology provides the direct measurements of the major types of body components. Though AGP was not used in the models described above, it is mainly due to statistical reasons. The AGP binding and IAM MB binding showed a significant correlation, so it was not possible to use both as independent variables in the regression equations. AGP binds also the positively charged compounds, however, there is a different steric hindrance for molecules that have bulky substitutions near the positive charge [62]. Although AGP can be found in human plasma at low concentrations (approximately 1.5 %) it may be significant in clinical investigations as its concentration depends on the disease state and can increase significantly [63]. Therefore compounds' strong binding to AGP should be avoided as it may cause variable free concentrations of the drug in patients with various diseases. The model to estimate total plasma protein binding ($\log k(PPB)$) includes the AGP binding as is shown by Equation 8 [64].

$$\log k(PPB) = 0.87 * \log k(HSA) + 0.17 * \log k(AGP) + 0.06 * cMR - 0.27 \quad (8)$$

$$n = 55 \quad r^2 = 0.85 \quad s = 0.36$$

cMR is the calculated molar refraction of the compounds related to the size of the molecules and accounts for the non-specific binding of the compounds to immunoglobulins in the plasma.

AGP also represents important cellular components such as glycoprotein in general. There has been observed overlapping binding between AGP and P-glycoprotein [65]. Also, the mucus in human airways is composed predominantly of glycoproteins. Several tissue binding models include the AGP binding, such as

mucus binding showed good correlation to AGP binding ($r^2 = 0.85$) [66] and lung tissue binding showed good correlations with the weighted sum of HSA and AGP bindings [67].

Conclusions

Established screening procedures in pharmaceutical drug discovery companies cause significant delays in getting a compound to market. One reason is that the initial discovery phase typically prioritises optimising discovery molecules to bind with high affinity to the target receptor. Drug analogues typically possess high receptor occupancy, which is anticipated to have better efficacy and selectivity, i.e., reduced off-target pharmacology. The insight lacking during this process is that all the potent analogues may not have the ADME properties to elicit sufficient free concentration of the drug near the receptor. We have presented an HPLC based technology by which the drug discovery process can be accelerated by chromatographic profiling of the analogues to model the *in vivo* drug disposition. The proposed methodology is able to identify compounds that have a greater probability of having acceptable *in vivo* properties. The methodology has been compared to Ligand Lipophilicity Efficiency (LLE) parameter that is used early in the lead optimization process. There is an inverse correlation between the maximum drug efficiency and $\text{clog}P$, thus LLE incorporates similar efficiency metrics as DEI. While $\text{clog}P$ can be easily calculated and the drug efficiency requires simple HPLC based measurements, the advantage is that it mimics the biological non-specific binding more accurately than calculated octanol/water lipophilicity. The measured IAM MB/PB incorporates the effect of charge and shape of the molecules on the binding to real body components which are not reflected in their distribution in octanol and water. The technology is suitable for estimating the tissue binding, plasma protein binding, volume of distribution, unbound volume of distribution, drug efficiency, promiscuity, phospholipidotic potential, etc. Therefore, this technology is recommended for use in early drug discovery programmes to aid the compound triage process so that only compounds with a higher probability of having good affinity along with good ADME properties are selected for progression to expensive animal studies. The technology is commercially available; the models have been published in a book titled "Physicochemical and Biomimetic Properties in Drug Discovery: Chromatographic Techniques for Lead Optimisation" [45] and are encouraged to be routinely used in the early drug discovery process.

The conclusion is that *in vivo* data should not be generated until the compounds have been analysed by chromatographic techniques, and only compounds that are predicted to have optimal *in vivo* properties should be progressed for further analysis. The proposed alternate drug discovery process should include (i) potency evaluation or receptor binding and (ii) predictive *in vivo* properties of each analogues. Only after both of these steps are completed should compounds be chosen for further development by extensive testing both *in vitro* and *in vivo*. Using this approach will eliminate numerous candidates from the pool of active analogues and has the potential to help save considerable amounts of time and money during the process of getting NCE's to market. Even if only 5-10 compounds are immediately eliminated as drug candidates, this potentially saves millions of dollars in the cost to get a drug to market.

References

- [1] E. Perola. *J. Med. Chem.* **53**(7) (2010) 2986–2997.
- [2] A. Cheng, D.J. Diller, S.L. Dixon, W.J. Egan, G. Lauri, K.M. Merz. *J. Comput. Chem.* **23**(1) (2002) 172–183.
- [3] H. Van de Waterbeemd, D.A. Smith, K. Beaumont, D.K. Walker. *J. Med. Chem.* **44**(9) (2001) 1313–1333.
- [4] I. Collins, P. Workman. *Nat. Chem. Biol.* **2**(12) (2006) 689–700.

- [5] A. Avdeef. *ADMET DMPK* **3(2)** (2015) 84–109.
- [6] J. Hughes, S. Rees, S. Kalindjian, K. Philpott. *Br. J. Pharmacol.* **162(6)** (2011) 1239–1249.
- [7] C.W. Murray, D.A. Erlanson, A.L. Hopkins, G.M. Keserü, P.D. Leeson, D.C. Rees, C.H. Reynolds, N.J. Richmond. *ACS Med. Chem. Lett.* **5(6)** (2014) 616–618.
- [8] A.L. Hopkins, G.M. Keserü, P.D. Leeson, D.C. Rees, C.H. Reynolds. *Nature Rev. Drug Discov.* **13(2)** (2014) 105–121.
- [9] J.D. Hughes, J. Blagg, D.A. Price, S. Bailey, G.A. DeCrescenzo, R.V. Devraj, et al. *Bioorg. Med. Chem. Lett.* **18(17)** (2008) 4872–4875.
- [10] A.A. Nava-Ocampo, A.M. Bello-Ramírez. *Clin. Exp. Pharmacol. Physiol.* **31** (2004) 116–118.
- [11] N.A. Meanwell. *Chem. Res. Toxicol.* **24(9)** (2011) 1420–1456.
- [12] T.J. Ritchie, S.J.F. Macdonald. *Drug Discov. Today* **14(21-22)** (2009) 1011–1020.
- [13] D. Smith, E.F. Schmid. *Curr. Opin. Drug Discov. Devel.* **9(1)** (2006) 38–46.
- [14] K.L. Valkó. *J. Pharm. Biomed. Anal.* **130** (2016) 35–54.
- [15] D. Stepensky. *Eur. J. Pharm. Sci.* **42(1-2)** (2011) 91–98.
- [16] D.A. Smith, L. Di, E.H. Kerns. *Nat. Rev. Drug Discov.* **9(12)** (2010) 929–939.
- [17] P.D. Dobson, D.B. Kell. *Nat. Rev. Discov.* **7(3)** (2008) 205–20.
- [18] S. Braggio, D. Montanari, T. Rossi, E. Ratti. *Expert Opin. Drug Discov.* **5** (2010) 609–618.
- [19] D. Montanari, E. Chiarparin, M.P. Gleeson, S. Braggio, R. Longhi, K. Valko K, et al. *Expert Opin. Drug Discov.* **6(9)** (2011) 913–920.
- [20] K.A. Youdim, A. Avdeef, N.J. Abbott. *Drug Discov. Today* **8(21)** (2003) 997–1003.
- [21] E.M. del Amo, L. Ghemtio, H. Xhaard, M. Yliperttula, A. Urtti, H. Kidron. *PLOS One* **8(10)** (2013) 1–12.
- [22] P. Thansandote, R.M. Harris, H.L. Dexter, G.L. Simpson, S. Pal, R.J. Upton, et al. *Bioorg. Med. Chem.* **23(2)** (2015) 322–327.
- [23] P.D. Leeson, B. Springthorpe. *Nat. Rev. Drug Discov.* **6(11)** (2007) 881–890.
- [24] B. Testa, P. Crivori, M. Reist, P. Carrupt. *Perspect. Drug Discovery Des.* **19** (2000) 179–211.
- [25] L. Huang, L. Berry, S. Ganga, B. Janosky, A. Chen, J. Roberts, et al. *Drug Metab. Dispos.* **38(2)** (2010) 223–331.
- [26] G.M. Keserü, G.M. Makara. *Nat. Rev. Drug Discov.* **8(3)** (2009) 203–212.
- [27] R.J. Young, D.V.S. Green, C.N. Luscombe, A.P. Hill. *Drug Discov. Today* **16(17-18)** (2011) 822–830.
- [28] C. Hansch, T. Fujita. ρ - σ - π Analysis. *J. Am. Chem. Soc.* **86(8)** (1964) 1616–1626.
- [29] M.D. Donovan. *J. Womens Health* **14(1)** (2005) 30–37.
- [30] J. Faulkner, D. McGibney, L. Chasseaud, J. Perry, I. Taylor. *Br. J. Clin. Pharmacol.* **22(1)** (1986) 21–25.
- [31] C. Pidgeon, S. Ong, H. Choi, H. Liu. *Anal. Chem.* **66(17)** (1994) 2701–2709.
- [32] C.Y. Yang, S.J. Cai, H. Liu, C. Pidgeon. *Adv. Drug Deliv. Rev.* **23(96)** (1996) 229–256.
- [33] C. Pidgeon. EP0408585A1 Immobilized Artificial Membranes, Int Pub Patent No WO 89/08/30, Filing: 21 February 1989.
- [34] S.K. Wiedmer, M.L. Riekkola, M.S. Jussila. *Trends Anal. Chem.* **23(8)** (2004) 562–582.
- [35] Y. Kumada, M. Nogami, N. Minami, M. Maehara, S. Katoh. *J. Chromatogr. A* **1080(1)** (2005) 22–28.
- [36] X.Y. Liu, Q. Yang, N. Kamo, J. Miyake. *J. Chromatogr. A* **913** (2001) 123–131.
- [37] K. Valko, S. Nunhuck, C. Bevan, M.H. Abraham, D.P. Reynolds. *J. Pharm. Sci.* **92(11)** (2003) 2236–2248.
- [38] J. Reilly, D. Etheridge, B. Everatt, Z. Jiang, C. Aldcroft, P. Wright, et al. *J. Liq. Chromatogr. Relat. Technol.* **34(4)** (2011) 317–327.
- [39] F. Beaudry, M. Coutu, N.K. Brown. *Biomed. Chromatogr.* **13(6)** (1999) 401–406.
- [40] M. Chrysanthakopoulos, T. Vallianatou, C. Giaginis, A. Tsantili-Kakoulidou. *Eur. J. Pharm. Sci.* **60** (2014) 24–31.
- [41] S. Taheri, L.P. Cogswell, A. Gent, G.R. Strichartz. *J. Pharmacol. Exp. Ther.* **304(1)** (2003) 71–80.

- [42] F. Hollosy, K. Valko, A. Hersey, S. Nunhuck, G. Keri, C. Bevan, et al. *J. Med. Chem.* **49(24)** (2006) 6958–6971.
- [43] K.L. Valkó, S.B. Nunhuck, A.P. Hill. *J. Pharm. Sci.* **100(3)** (2011) 849–862.
- [44] X. Zhao, W. Chen, Z. Zhou, Q. Wang, Z. Liu, R. Moaddel, et al. *J. Chromatogr. A* **1407** (2015) 176–183.
- [45] K. Valko. *Physicochemical and Biomimetic Properties in Drug Discovery: Chromatographic techniques for Lead Optimization*. Wiley Hoboken NJ; 2014. 226 p.
- [46] K.M. Wasan, D.R. Brocks, S.D. Lee, K. Sachs-Barrable, S.J. Thornton. *Nat. Rev. Drug Discov.* **7(1)** (2008) 84–99.
- [47] A. Casartelli, M. Bonato, P. Cristofori, F. Crivellente, G. Dal Negro, I. Masotto, et al. *Cell Biol. Toxicol.* **19(3)** (2003) 161–176.
- [48] L.J. Gordon, M. Allen, P. Artursson, M.M. Hann, B.J. Leavens, A. Mateus, et al. *J. Biomol. Screen.* **21(2)** (2016) 156–164.
- [49] K.M. Page. *Mol. Pharm.* **13(2)** (2016) 609–620.
- [50] K. Tam. *ADMET DMPK* **1(4)** (2013) 63–75.
- [51] K. Valko, E. Chiarparin, S. Nunhuck, D. Montanari. *J. Pharm. Sci.* **101(11)** (2012) 4155–4169.
- [52] K. Valko, C.M. Du, C.D. Bevan, D.P. Reynolds, M.H. Abraham, *J. Pharm. Sci.* **89(8)** (2000) 1085–1096.
- [53] G. Russo, L. Grumetto, F. Barbato, G. Vistoli, A. Pedretti. *Eur. J. Pharm. Sci.* **99** (2017) 173–184.
- [54] G. Colmenarejo. *Med. Res. Rev.* **23(3)** (2003) 275–301.
- [55] G. Lambrinidis, T. Vallianatou, A. Tsantili-Kakoulidou. *Adv. Drug Deliv. Rev.* **86** (2015) 27–45.
- [56] P.N. Mortenson, C.W. Murray. *J. Comput. Aided Mol. Des.* **25(7)** (2011) 663–667.
- [57] U.M. Hanumegowda, G. Wenke, A. Regueiro-Ren, R. Yordanova, J.P. Corradi, S.P. Adams. *Chem. Res. Toxicol.* **23(4)** (2010) 749–755.
- [58] D. Price, J. Blagg, L. Jones, N. Greene, T. Wager. *Expert Opin. Drug Metab. Toxicol.* **5(8)** (2009) 921–931.
- [59] A. Casartelli, A. Lanzoni, R. Comelli, F. Crivellente, R. Defazio, R. Dorigatti, et al. *Toxicol. Pathol.* **39(2)** (2011) 361–371.
- [60] L.J. Gordon, M. Allen, P. Artursson, M.M. Hann, B.J. Leavens, A. Mateus, et al. *J. Biomol. Screen.* **21(2)** 2016 156–164.
- [61] D. Stepensky. *Expert Opin. Drug Metab. Toxicol.* **7(10)** (2011) 1233–1243.
- [62] R. Kaliszan, A. Nasal, M. Turowski. *Biomed. Chromatogr.* **9(5)** (1995) 211–215.
- [63] T. Fournier, N. Medjoubi, D. Porquet. *Biochim. Biophys. Acta* **1482** (2000) 157–171.
- [64] K. Valko. *Physicochemical and Biomimetic Properties in Drug Discovery: Chromatographic Techniques for Lead Optimization*. Wiley Hoboken NJ, (2014), Chapter 11, p. 294–310.
- [65] F. Zsila. *Curr. Drug Metab.* **8** (2007) 563–593.
- [66] K. Valko. *Physicochemical and Biomimetic Properties in Drug Discovery: Chromatographic Techniques for Lead Optimization*. Wiley Hoboken NJ, (2014) Chapter 11, p. 295.
- [67] K. Valko. *Physicochemical and Biomimetic Properties in Drug Discovery: Chromatographic Techniques for Lead Optimization*. Wiley Hoboken NJ, (2014), Chapter 11, p. 296.

Appendix

Table A1. The in vivo human data for the investigated marketed drugs. Training set marked from the V_d model [42].

DRUG	Test set / training set	Actual daily dose	pIC 50	Dosing /day	In vivo human V_{dss} (L/kg)	in vivo log V_{dss}	in vivo V_{du} (L/kg)	in vivo log V_{du}	In vivo Cl ml/min/kg	in vivo log Cl	$t_{1/2}$ (h)	Log $t_{1/2}$ (h)
ABACAVIR	Test	600	7.2	2	0.84	-0.08	1.68	0.23	13.00	1.11	1.00	0.00
ACEBUTOLOL HYDROCHLORIDE	Test	400	6.8	2	1.7	0.23	2.30	0.36	10.00	1.00	3.50	0.54
ACETYLSALICYLIC ACID	Train.	1200	5.5	3	0.22	-0.66	0.32	-0.49	12.00	1.08		
ACRIVASTINE	Test	32	8.5	4							1.50	0.18
ALBUTEROL SULFATE	Test	8	7.4	4	1.9	0.28	2.07	0.31	7.80	0.89	2.40	0.38
ALLOPURINOL	Test	300	5.3	1	0.58	-0.24	0.60	-0.22	11.00	1.04	0.80	-0.10
ALOSETRON HYDROCHLORIDE	Train.	1	7.3	2	1.1	0.04	6.11	0.79	8.70	0.94	1.60	0.20
AMILORIDE HYDROCHLORIDE	Test	5	5.5	1	5	0.70					7.50	0.88
AMINO-GLUTETHIMIDE	Test	500	4.9	2							12.50	1.10
AMITRIPTYLINE HYDROCHLORIDE	Test	50	6.2	1	8.7	0.94	124.29	2.09	6.10	0.79	17.00	1.23
AMOXAPINE	Train.	300	6.5	3								
ARIPIRAZOLE	Test	10	9.7	1	4.9	0.69	490.00	2.69	0.83	-0.08	75.00	1.88
ATOMOXETINE HYDROCHLORIDE1	Test	40	8.7	1	0.85	-0.07	42.50	1.63	9.30	0.97	5.20	0.72
BENDRO-FLUMETHIAZIDE	Test	3	3.4	1							8.50	0.93
BICALUTAMIDE	Test	50	6.1	1							144.00	2.16
BUPROPION HYDROCHLORIDE	Test	300	6.3	1							24.00	1.38
CABERGOLINE	Test	0	10	0					45.71	1.66	65.00	1.81
CAFFEINE	Test	150	4.7	3	0.63	-0.20	0.98	-0.01	1.40	0.15	4.90	0.69
CANDESARTAN CILEXETIL	Test	8	10.5	1	0.13	-0.89	13.00	1.11	0.37	-0.43	9.00	0.95
CARBAMAZEPINE	Train.	800	4.6	1							17.00	1.23
CELECOXIB	Test	400	8.5	2	6.13	0.79	204.33	2.31	6.59	0.82	11.00	1.04
CILOSTAZOL	Test	200	6.7	2							12.00	1.08
CITALOPRAM HYDROBROMIDE	Test	20	8.3	1	12	1.08	60.00	1.78	4.30	0.63	33.00	1.52
CLOMIPRAMINE HYDROCHLORIDE	Test	25	7.9	1	13	1.11	433.33	2.64	8.20	0.91	26.00	1.41
CLONIDINE HYDROCHLORIDE	Train.	0	8.5	1	3.3	0.52	5.89	0.77	4.00	0.60	7.60	0.88
DAPSONE	Test	100	4.8	1	0.83	-0.08	3.32	0.52	0.48	-0.32	22.00	1.34
DESLOMATADINE	Test	5	9.4	1							50.00	1.70

DIAZOXIDE	Train.	150	4.7	3	0.21	-0.68	3.50	0.54	0.06	-1.22	48.00	1.68
DIDANOSINE	Test	250	8	2	0.77	-0.11	0.81	-0.09	11.00	1.04	1.40	0.15
DIFLUNISAL	Train.	1000	4.2	2	0.1	-1.00			0.10	-1.00	10.00	1.00
DIPHENHYDRAMINE HYDROCHLORIDE	Train.	75	8.1	3	6.5	0.81	34.21	1.53	9.80	0.99	9.30	0.97
DIPYRIDAMOLE	Train.	200	6.7	2	1.75	0.24	175.00	2.24	3.00	0.48	0.70	-0.15
DOMPERIDONE	Test	30	9.8	3	3.4	0.53	42.50	1.63	9.50	0.98	7.50	0.88
DONEPEZIL HYDROCHLORIDE	Test	5	8.2	1	12	1.08	300.00	2.48	2.17	0.34	70.00	1.85
EFAVIRENZ	Test	600	8.9	1							47.00	1.67
ETODOLAC	Test	600	6.2	2	0.39	-0.41	39.00	1.59	0.82	-0.09	7.30	0.86
FELBAMATE	Train.	1200	3.4	3	0.76	-0.12	1.09	0.04	0.50	-0.30	22.00	1.34
FELODIPINE	Train.	5	9.8	1	4.4	0.64			11.00	1.04	10.00	1.00
FEXOFENADINE HYDROCHLORIDE	Test	60	7.3	2							14.40	1.16
FINASTERIDE	Train.	5	7.3	1	0.89	-0.05	5.56	0.75	4.70	0.67	3.00	0.48
FLUOXETINE HYDROCHLORIDE	Train.	60	8.6	1	32.5	1.51	541.67	2.73			48.00	1.68
FLURBIPROFEN	Train.	200	6.2	4	0.12	-0.92					5.00	0.70
FLUTAMIDE	Test	750	5.9	3							6.00	0.78
FLUVOXAMINE MALEATE	Test	50	8.3	1	25	1.40	125.00	2.10			15.60	1.19
FUROSEMIDE	Train.	80	5	2	0.12	-0.92	12.00	1.08	1.60	0.20	2.50	0.40
GLIBENCLAMIDE	Test	3	5.3	1	0.13	-0.89	13.00	1.11	1.30	0.11	1.60	0.20
GLIMEPIRIDE	Test	1	5.4	1	0.19	-0.72	19.00	1.28	0.50	-0.30	10.00	1.00
GLIPIZIDE	Train.	3	5.5	1	0.16	-0.80	8.00	0.90	0.56	-0.25	3.30	0.52
GRANISETRON HYDROCHLORIDE	Test	2	9.9	2	3.7	0.57	10.57	1.02	9.10	0.96	5.20	0.72
GUANABENZ ACETATE	Test	8	8.2	2							6.00	0.78
HALOPERIDOL	Test	2	10	2	17	1.23	212.50	2.33	7.80	0.89	35.00	1.54
HYDROCHLOROTHIA ZIDE	Test	50	4.7	2							8.00	0.90
IMIPRAMINE HYDROCHLORIDE	Train.	75	6.6	1	12	1.08	150.00	2.18	13.00	1.11	16.00	1.20
INDAPAMIDE	Test	1	4.2	1							14.00	1.15
INDOMETHACIN	Train.	75	6.5	3	0.1	-1.00	10.00	1.00	1.30	0.11	1.40	0.15
IRBESARTAN	Test	150	9.3	1	0.94	-0.03	9.40	0.97	2.30	0.36	14.00	1.15
ISRADIPINE	Test	5	6.6	2	1.5	0.18	37.50	1.57	26.00	1.41	3.30	0.52
KETOCONAZOLE	Train.	200	4.7	1							2.00	0.30
KETOPROFEN	Train.	225	7.6	3	0.13	-0.89	1.63	0.21	1.60	0.20	2.10	0.32
LAMOTRIGINE	Test	25	4	1	1.1	0.04	2.44	0.39	0.58	-0.24	25.00	1.40
LANSOPRAZOLE	Test	15	7.1	1	0.28	-0.55	14.00	1.15	4.40	0.64	1.00	0.00
LEFLUNOMIDE	Test	100	4.9	1	0.13	-0.89	13.00	1.11			336.00	2.53

LETROZOLE	Test	3	7.9	1	1.9	0.28	4.63	0.67	0.57	-0.24	45.00	1.65
LORAZEPAM	Train.	3	8.9	3	1.3	0.11	14.44	1.16	1.00	0.00	17.00	1.23
LOVASTATIN	Test	10	9.5	1	0.87	-0.06	21.75	1.34	7.20	0.86	1.40	0.15
LOXAPINE SUCCINATE	Test	40	8.3	2							4.00	0.60
MAPROTILINE HYDROCHLORIDE	Train.	75	4.4	3	45	1.65	409.09	2.61	14.00	1.15	51.00	1.71
MEBENDAZOLE	Train.	200	6.7	2	1.2	0.08	13.33	1.12	15.00	1.18	1.10	0.04
MERCAPTOPYRINE	Test	3	4.8	1	1	0.00	1.18	0.07	15.00	1.18	1.00	0.00
METHYL- PREDNISOLONE	Train.	4	6.3	1	1.2	0.08	5.22	0.72	6.10	0.79	2.30	0.36
METOCLOPRAMIDE HYDROCHLORIDE	Test	20	8.4	2	3.2	0.51	5.33	0.73	5.70	0.76	7.20	0.86
METOLAZONE	Test	3	5.7	1							14.00	1.15
MIANSERIN	Train.	60	8.1	2							13.50	1.13
MIBEFRADIL DIHYDROCHLORIDE	Test	50	6.2	1	3.1	0.49	310.00	2.49	4.00	0.60	13.00	1.11
MIFEPRISTONE	Test	600	8	1							18.00	1.26
MYCOPHENOLIC ACID	Test	1440	8	2	0.77	-0.11	38.50	1.59	2.00	0.30	12.00	1.08
NADOLOL	Train.	40	8.9	1	1.9	0.28	13.57	1.13	2.90	0.46	9.20	0.96
NAPROXEN	Train.	1000	5.2	2							15.00	1.18
NEOSTIGMINE BROMIDE	Train.	15	7.4	1	0.74	-0.13			9.20	0.96	1.30	0.11
NEVIRAPINE	Test	200	8	1	1.3	0.11	4.06	0.61	0.30	-0.52	53.00	1.72
NICARDIPINE HYDROCHLORIDE	Train.	60	5.6	2	1	0.00	100.00	2.00	11.00	1.04	4.10	0.61
NIMESULIDE	Test	400	4.4	2							2.80	0.45
NIMODIPINE	Test	120	9.6	4	1.1	0.04	55.00	1.74	15.00	1.18	1.30	0.11
NISOLDIPINE	Test	20	9.8	1	5.5	0.74			15.00	1.18	11.00	1.04
NITRENDIPINE	test	20	7.6	2	6.1	0.79	305.0	2.48	25.00	1.40	8.20	0.91
NORTRIPTYLINE HYDROCHLORIDE	Train.	75	9	3	22	1.34	183.33	2.26	10.00	1.00	30.00	1.48
OLANZAPINE	Test	10	7.5	1	14.3	1.16	204.29	2.31	7.14	0.85	37.50	1.57
PENTOXIFYLLINE	Train.	800	3.7	2	1.8	0.26	6.00	0.78	39.00	1.59	1.20	0.08
PERGOLIDE MESYLATE	Test	0	8.9	1							27.00	1.43
PHENYTOIN	Train.	90	4.2	1							22.00	1.34
PIMOZIDE	Test	8	9.6	2							29.30	1.47
PIOGLITAZONE HYDROCHLORIDE	Test	15	4.5	1	0.63	-0.20	63.00	1.80			5.00	0.70
PIROXICAM	Train.	20	6.7	1	0.14	-0.85	2.33	0.37			58.00	1.76
PRAVASTATIN SODIUM	Test	40	8.2	1	0.46	-0.34	0.92	-0.04	14.00	1.15	0.80	-0.10
PRAZOSIN HYDROCHLORIDE	Train.	2	8.9	3	0.73	-0.14	12.17	1.09	4.70	0.67	2.00	0.30
PRIMAQUINE PHOSPHATE	Test	15	5.4	1	4	0.60			5.80	0.76	7.10	0.85

PROBENECID	Train.	1000	3.8	2	0.13	-0.89	1.00	0.00	0.25	-0.60	5.90	0.77
PROCHLORPERAZIN E MALEATE	Test	15	8.5	3	22	1.34			16.00	1.20	9.00	0.95
PROCYCLIDINE HYDROCHLORIDE	Test	8	8.6	3	0.74	-0.13			0.86	-0.07	12.00	1.08
PROMETHAZINE HYDROCHLORIDE	Test	50	8.2	2	14	1.15	155.56	2.19	14.00	1.15	14.00	1.15
PROPAFENONE HYDROCHLORIDE	Test	450	5.7	3	2.2	0.34	55.00	1.74	16.00	1.20	2.10	0.32
PROPRANOLOL HCL	Train.	160	9.4	2	3.1	0.49	23.85	1.38	12.00	1.08	3.40	0.53
PROTRIPTYLINE HYDROCHLORIDE	Test	15	5.6	3	22	1.34						
QUININE SULFATE	Train.	1800	6.3	6	1.8	0.26	6.00	0.78	1.90	0.28	11.00	1.04
RILUZOLE	Test	100	4.4	2							12.00	1.08
ROXITHROMYCIN	Test	450	6.8	3			0.00				12.00	1.08
SAQUINAVIR	Test	2000	8.3	2	3.6	0.56	120.00	2.08	13.00	1.11	13.00	1.11
SIMVASTATIN	Test	40	8.4	1							3.00	0.48
SULFINPYRAZONE	Train.	100	3.3	1	0.12	-0.92	6.00	0.78	0.34	-0.47	6.20	0.79
SUMATRIPTAN	Test	75	8.1	3	1.7	0.23	2.05	0.31	19.00	1.28	1.70	0.23
TAMSULOSIN HYDROCHLORIDE	Test	2	11	2	0.21	-0.68	21.00	1.32	0.62	-0.21	6.80	0.83
TRAZODONE HYDROCHLORIDE	Train.	150	6.3	1	0.52	-0.28			1.40	0.15	7.30	0.86
VENLAFAXINE HYDROCHLORIDE	Test	75	7.7	2	4.4	0.64	6.03	0.78	14.00	1.15	5.00	0.70
VERAPAMIL HYDROCHLORIDE	Test	120	6.9	3	3.7	0.57	41.11	1.61	18.00	1.26	2.80	0.45

Table A2. Measured biomimetic properties and estimated volume of distribution, unbound volume of distribution based on the published models. %HSA binding is obtained from the $\log t_R$ vs $\log k(\text{HSA})$ calibration plot using $\% \text{HSA} = 101 * 10^{\log k(\text{HSA})} / (1 + 10^{\log k(\text{HSA})})$, $\log K(\text{HSA}) = \exp(\log k(\text{HSA}))$; $\log K(\text{IAM})$ obtained from measured IAM MB as described by Equation (1); IAM MB/PB DE_{\max} is calculated from V_{du} as $100/V_{du}$ where $\log V_{du}$ is obtained as a sum of $\log K(\text{IAM})$ and $\log K(\text{HSA})$ according to Equation (4); IAM MB/PB $\log V_{dss}$ is obtained from the difference between $\log K(\text{IAM})$ and $\log K(\text{HSA})$ as described by Equation 3. The test/training marks are based whether it was used in the model building for V_{du} [43].

DRUG	Test or training set of compound	%HSA binding	$\log K(\text{HSA})$ Converted to $\log P$ scale	$\log K(\text{IAM})$ converted to $\log P$ scale	IAM MB/PB DE_{\max} (%)	IAM MB/PB $\log V_{du}$	IAM MB/PB $\log V_{dss}$	Acid/base character
ABACAVIR	test	31.9	0.71	1.77	60.9	0.21	-0.04	Weak Base
ACEBUTOLOL HYDROCHLORIDE	test	32.7	0.73	1.59	72.1	0.13	-0.12	Basic
ACETYLSALICYLIC ACID	test	66.4	1.33					Acidic
ACRIVASTINE	test	82.5	1.91	2.68	13.2	0.87	0.10	Weak Base

ALBUTEROL SULFATE	test	22	0.57	1.55	81.6	0.08	-0.10	Basic
ALLOPURINOL		19.2	0.53	2	54.9	0.26	0.10	Acidic
ALOSETRON HYDROCHLORIDE	test	75.5	1.60	2.68	15.8	0.80	0.17	Weak Base
AMILORIDE HYDROCHLORIDE	training	38.6	0.81	2.56	27.3	0.57	0.29	Acidic
AMINOGLUTETHIMIDE	training	25.9	0.63	1.53	81	0.08	-0.13	Weak Base
AMITRIPTYLINE HYDROCHLORIDE	test	90.1	2.50	6.3	0.308	2.56	1.56	Basic
AMOXAPINE	test	88.4	2.33	6.64	0.24	2.67	1.75	Basic
ARIPIRAZOLE	test	97.8	4.42	6.08	0.129	2.91	1.04	Basic
ATOMOXETINE HYDROCHLORIDE1	test	87.5	2.25	5.28	0.922	2.07	1.17	Basic
BENDROFLUMETHIAZIDE	test	64.4	1.28	2.95	12.7	0.84	0.36	Weak Acid
BICALUTAMIDE	test	96.8	3.91	3.21	2.66	1.56	-0.11	Neutral
BUPROPION HYDROCHLORIDE	test	73.9	1.55	3.21	9.7	1.02	0.41	Basic
CABERGOLINE	test	83.6	1.98	6.41	0.366	2.49	1.73	Basic
CAFFEINE	test	26.8	0.64	1.22	108	-0.05	-0.26	Neutral
CANDESARTAN CILEXETIL	test	97.9	4.48	3.8	1.07	1.94	0.03	Acidic
CARBAMAZEPINE	test	79.9	1.78	2.34	19.7	0.70	-0.02	Neutral
CELECOXIB	test	97.1	4.04	3.9	1.24	1.89	0.17	Neutral
CILOSTAZOL	test	89.9	2.48	3.02	6.97	1.15	0.12	
CITALOPRAM HYDROBROMIDE	test	72.4	1.50	4.85	2.12	1.71	1.14	Basic
CLOMIPRAMINE HYDROCHLORIDE	test	94.4	3.18	7.6	0.06	3.28	1.99	Basic
CLONIDINE HYDROCHLORIDE	test	37.7	0.80	1.96	48.9	0.31	0.03	Basic
DAPSONE	test	80.6	1.82	2.07	25	0.59	-0.15	Neutral
DESLORATADINE	test	88.5	2.34	6.13	0.39	2.45	1.52	Basic
DIAZOXIDE	training	77.6	1.68	2.05	27.3	0.55	-0.13	Acidic
DIDANOSINE	test	27.5	0.65					Weak Acid
DIFLUNISAL	test	98.8	5.22	2.49	2.57	1.55	-0.71	Acidic
DIPHENHYDRAMINE HYDROCHLORIDE	test	68.7	1.39	2.98	13.3	0.88	0.35	Basic
DIPYRIDAMOLE	test	88.2	2.31	4.03	2.93	1.54	0.60	Weak Base
DOMPERIDONE	test	92.2	2.77	3.96	2.43	1.62	0.47	Basic
DONEPEZIL HYDROCHLORIDE	test	86.1	2.14	3.68	4.45	1.36	0.49	Basic
EFAVIRENZ	test	97.3	4.14	4.34	0.777	2.10	0.34	
ETODOLAC	test	95.6	3.48	2.51	6.52	1.16	-0.32	Acidic
FELBAMATE	test	68.7	1.39	1.76	42.3	0.36	-0.19	Neutral
FELODIPINE	test	95.9	3.58	4.45	0.965	2.02	0.51	Neutral

FEXOFENADINE HYDROCHLORIDE	test	74.1	1.55	2.64	16.6	0.77	0.16	Basic
FINASTERIDE	test	88.4	2.33	3.34	5.55	1.25	0.30	
FLUOXETINE HYDROCHLORIDE	test	91.2	2.63	6.19	0.305	2.55	1.48	Basic
FLURBIPROFEN	test	98.6	5.02	1.99	4.77	1.29	-0.89	Acidic
FLUTAMIDE	test	94.3	3.15	3.48	3.11	1.50	0.18	Neutral
FLUVOXAMINE MALEATE	test	72.3	1.49	5.15	1.59	1.84	1.28	Basic
FUROSEMIDE	test	89.7	2.46	2.14	12.4	0.77	-0.26	Acidic
GLIBENCLAMIDE	test	98	4.55	2.7	2.99	1.49	-0.47	Acidic
GLIMEPIRIDE	test	98	4.55	2.53	3.61	1.41	-0.55	Acidic
GLIPIZIDE	test	95.8	3.54	1.83	12	0.88	-0.63	Acidic
GRANISETRON HYDROCHLORIDE	test	69	1.40	4.34	3.57	1.47	0.94	Basic
GUANABENZ ACETATE	test	88.1	2.30	4.85	1.36	1.90	0.97	Basic
HALOPERIDOL	test	90.4	2.54	4.6	1.46	1.84	0.81	Basic
HYDROCHLOROTHIAZIDE	test	45.4	0.92	1.62	63.3	0.19	-0.15	
IMIPRAMINE HYDROCHLORIDE	test	86.3	2.16	4.23	2.63	1.59	0.73	Basic
INDAPAMIDE	test	75.1	1.59	2.6	17.1	0.76	0.13	Weak Acid
INDOMETACIN	test	98.6	5.02	2.34	3.33	1.44	-0.74	Acidic
IRBESARTAN	test	96.1	3.64	2.17	8.18	1.05	-0.51	Acidic
ISRADIPINE	test	94.4	3.18	3.48	3.05	1.51	0.17	Neutral
KETOCONAZOLE	training	94.6	3.22	3.59	2.69	1.56	0.21	Weak Base
KETOPROFEN	test	98.4	4.85	2.18	4.3	1.33	-0.77	Acidic
LAMOTRIGINE	test	59.5	1.17	1.99	38.5	0.40	-0.04	Weak Base
LANSOPRAZOLE	test	90.5	2.55	2.66	9.45	1.01	-0.05	
LEFLUNOMIDE	test	92.6	2.84	3.37	4.07	1.38	0.20	Neutral
LETROZOLE	test	59.3	1.17	2.42	25.7	0.59	0.15	Neutral
LORAZEPAM	test	91.1	2.62	3.16	5.67	1.24	0.15	Neutral
LOVASTATIN	test	95.5	3.45	4.09	1.47	1.83	0.38	Neutral
LOXAPINE SUCCINATE	test	92.7	2.85	5.28	0.658	2.21	1.04	Basic
MAPROTILINE HYDROCHLORIDE	training	86	2.13	6.7	0.25	2.65	1.82	Basic
MEBENDAZOLE	test	92.9	2.89	3.07	5.25	1.26	0.06	Weak Base
MERCAPTOPYRINE	test	41.2	0.85					
METHYLPREDNISOLONE	test	71.9	1.48	2.6	18.2	0.74	0.16	Neutral
METOCLOPRAMIDE HYDROCHLORIDE	test	58.9	1.16	3.54	8.87	1.07	0.64	Basic
METOLAZONE	test	83.8	1.99	2.49	15.2	0.81	0.00	Neutral
MIANSERIN	test	91.9	2.73	5.47	0.595	2.26	1.15	Basic
MIBEFRADIL DIHYDROCHLORIDE	test	93.6	3.01	6.3	0.231	2.68	1.45	Basic
MIFEPRISTONE	test	95.5	3.45	4.2	1.33	1.88	0.43	

MYCOPHENOLIC ACID	test	95.5	3.45	1.83	12.7	0.86	-0.61	Acidic
NADOLOL	test	39.7	0.83	1.76	58.5	0.23	-0.07	
NAPROXEN	test	99.9	7.09	1.96	1.55	1.75	-1.36	Acidic
NEOSTIGMINE BROMIDE	test	87.6	2.26	1.68	28.1	0.52	-0.42	Basic
NEVIRAPINE	test	54	1.06	1.89	45	0.34	-0.06	Neutral
NICARDIPINE HYDROCHLORIDE	test	95.8	3.54	4.23	1.21	1.91	0.42	Weak Base
NIMESULIDE	test	98	4.55	2.32	4.4	1.32	-0.64	Acidic
NIMODIPINE	test	92	2.74	3.09	5.64	1.24	0.10	Neutral
NISOLDIPINE	test	91	2.61	3.16	5.67	1.24	0.16	Neutral
NITRENDIPINE	test	93.9	3.07	3.59	2.88	1.53	0.24	Neutral
NORTRIPTYLINE HYDROCHLORIDE	training	86.2	2.15	5.66	0.673	2.21	1.36	Basic
OLANZAPINE	test	86.2	2.15	5.06	1.2	1.95	1.09	Basic
PENTOXIFYLLINE	test	25.9	0.63	1.47	85.5	0.06	-0.15	Neutral
PERGOLIDE MESYLATE	test	85.2	2.08	5.71	0.672	2.21	1.40	Basic
PHENYTOIN	test	83.4	1.97	2.51	15.1	0.81	0.01	Weak Acid
PIMOZIDE	test	98.6	5.02	5.61	0.142	2.85	0.70	Basic
PIOGLITAZONE HYDROCHLORIDE	test	97.9	4.48	2.76	2.97	1.50	-0.43	
PIROXICAM	test	97.3	4.14	1.9	8.14	1.05	-0.73	Acidic
PRAVASTATIN SODIUM	test	40.3	0.84	1.83	54	0.26	-0.04	Acidic
PRAZOSIN HYDROCHLORIDE	test	85.2	2.08	2.47	14.6	0.82	-0.03	Weak Base
PRIMAQUINE PHOSPHATE	test	79.2	1.75	4.6	2.31	1.66	0.98	Basic
PROBENECID	training	95.4	3.43	1.81	13.2	0.85	-0.62	Acidic
PROCHLORPERAZINE MALEATE	test	96.9	3.95	7.67	0.037	3.49	1.85	Basic
PROCYCLIDINE HYDROCHLORIDE	test	86.1	2.14	4.49	1.72	1.70	0.84	Neutral
PROMETHAZINE HYDROCHLORIDE	test	92.5	2.82	7.2	0.107	3.02	1.89	Basic
PROPAFENONE HYDROCHLORIDE	training	88	2.29	4.38	2.1	1.69	0.76	Basic
PROPRANOLOL HCL	test	72.7	1.51	4.45	3.04	1.54	0.97	Basic
PROTRIPTYLINE HYDROCHLORIDE	test	83.8	1.99	5.42	0.929	2.07	1.29	Basic
QUININE SULFATE	test	78.1	1.70	5.19	1.35	1.90	1.25	Basic
RILUZOLE	test	94.2	3.13	3.29	3.71	1.41	0.10	Weak Base
ROXITHROMYCIN	test	46.6	0.93	5.37	1.88	1.80	1.50	
SAQUINAVIR	test	95.2	3.37	3.77	2.07	1.68	0.26	Weak Base
SIMVASTATIN	test	96.6	3.82	4.49	0.823	2.09	0.47	
SULFINPYRAZONE	training	97.2	4.09	2.11	6.83	1.13	-0.63	Acidic
SUMATRIPTAN	test	28	0.66	2.68	26.5	0.58	0.37	Basic

TAMSULOSIN HYDROCHLORIDE	test	68.9	1.39	2.84	14.8	0.82	0.28	Basic
TRAZODONE HYDROCHLORIDE	test	92	2.74	3.04	5.81	1.22	0.07	Weak Base
VENLAFAXINE HYDROCHLORIDE	test	35	0.76	3.19	15.5	0.83	0.58	Basic
VERAPAMIL HYDROCHLORIDE	test	88.1	2.30	3.59	3.93	1.35	0.41	Basic
ZAFIRLUKAST	test	99.1	5.57	3.67	0.789	2.14	-0.27	Acidic
ZALCITABINE	test	23.6	0.60					Zwitterionic
ZIDOVUDINE	test	11.9	0.42	1.17	127	-0.12	-0.24	Weak Acid
ZILEUTON	training	89.7	2.46	2.53	10.46	0.93	-0.09	Neutral
ZIPRASIDONE HYDROCHLORIDE	training	97.2	4.09	4.64	0.596	2.22	0.48	Weak Base
ZOLMITRIPTAN	training	61.4	1.21	2.78	16.3	0.75	0.30	Basic

©2017 by the authors; licensee IAPC, Zagreb, Croatia. This article is an open-access article distributed under the terms and conditions of the Creative Commons Attribution license (<http://creativecommons.org/licenses/by/3.0/>) 